The Journal of Immunology

Design and Validation of a Novel Generic Platform for the Production of Tetravalent IgG1-like Bispecific Antibodies

Josée Golay, Sylvie Choblet, Justyna Iwaszkiewicz, Pierre Cérutti, Annick Ozil, Séverine Loisel, Martine Pugnière, Greta Ubiali, Vincent Zoete, Olivier Michielin, Christian Berthou, Jean Kadouche, Jean-Pierre Mach and Martine Duonor-Cérutti

J Immunol 2016; 196:3199-3211; Prepublished online 26 February 2016;
doi: 10.4049/jimmunol.1501592
http://www.jimmunol.org/content/196/7/3199

The Journal of Immunology is published twice each month by
The American Association of Immunologists, Inc.,
1451 Rockville Pike, Suite 650, Rockville, MD 20852

Print ISSN: 0022-1767 Online ISSN: 1550-6606.

Design and Validation of a Novel Generic Platform for the Production of Tetravalent IgG1-like Bispecific Antibodies

Josée Golay,* Sylvie Choblet,[†,1] Justyna Iwaszkiewicz,[‡,1] Pierre Cérutti,[†] Annick Ozil,[†] Séverine Loisel,[§] Martine Pugnière,[¶] Greta Ubiali,* Vincent Zoete,[‡] Olivier Michielin,[‡,‖,#] Christian Berthou, Jean Kadouche,[††,‡‡] Jean-Pierre Mach,[§§,¶¶] and Martine Duonor-Cérutti[†]**

We have designed and validated a novel generic platform for production of tetravalent IgG1-like chimeric bispecific Abs. The VH-CH1-hinge domains of mAb2 are fused through a peptidic linker to the N terminus of mAb1 H chain, and paired mutations at the CH1-CL interface mAb1 are introduced that force the correct pairing of the two different free L chains. Two different sets of these CH1-CL interface mutations, called CR3 and MUT4, were designed and tested, and prototypic bispecific Abs directed against CD5 and HLA-DR were produced (CD5xDR). Two different hinge sequences between mAb1 and mAb2 were also tested in the CD5xDR-CR3 or -MUT4 background, leading to bispecific Ab (BsAbs) with a more rigid or flexible structure. All four Abs produced bound with good specificity and affinity to CD5 and HLA-DR present either on the same target or on different cells. Indeed, the BsAbs were able to efficiently redirect killing of HLA-DR$^+$ leukemic cells by human CD5$^+$ cytokine-induced killer T cells. Finally, all BsAbs had a functional Fc, as shown by their capacity to activate human complement and NK cells and to mediate phagocytosis. CD5xDR-CR3 was chosen as the best format because it had overall the highest functional activity and was very stable in vitro in both neutral buffer and in serum. In vivo, CD5xDR-CR3 was shown to have significant therapeutic activity in a xenograft model of human leukemia. ***The Journal of Immunology*****, 2016, 196: 3199–3211.**

Therapeutic mAbs have recently shown a great potential in human cancer treatment (1). However, their activities as monotherapy are often insufficient to produce a lasting benefit. Several approaches have been used to enhance their efficacy, the most common being conjugation with toxins or drugs (2) and the development of bispecific Abs (BsAbs) (3, 4). Indeed, BsAbs are promising immunotherapy tools that have improved therapeutic activity through different mechanisms (i.e., by cross-linking 1) two distinct cell surface Ags presented on the same cell (normal or malignant), 2) Ags expressed on different cells, a tumor cell, and an immune cell thus modulating immunity either positively or negatively, 3) a molecule on a target cell and a soluble mediator, or 4) two soluble mediators). Furthermore, BsAbs may or may not have an Fc capable of bridging an FcR bearing effector cell to the cancer target and of providing greater stability in vivo.

However, BsAbs are difficult to produce and several strategies have been developed for their generation, including chemical conjugation (5, 6), fusion of two hybridomas (quadroma) (7) and more effectively genetic engineering (4, 8). Some of these engineered multispecific Abs result from the fusion of fragment variable (Fv) or single-chain variable fragment (scFv), generating small molecules lacking Fc, with short serum half life and unable to activate immune effectors (4). Nonetheless, several of these BsAb fragments are approved or in advanced clinical trials, such as the bispecific T cell engagers, designed to redirect T cell on tumor cells via the binding to CD3 and a tumor surface Ag (9, 10), the tetravalent tandem diabody (11), and the Dual-Affinity-RetargeTing (12). Combinations of nanobodies isolated from camelidae H chain Abs are also used to generate bi- or multispecific molecules (13).

*Centro di Terapia Cellulare "G. Lanzani," Divisione di Ematologia, Azienda Ospedaliera Papa Giovanni XXIII, 24122 Bergamo, Italy; [†]Centre National de la Recherche Scientifique UPS3044 "Baculovirus et Thérapie," F-30380 Saint-Christol-Lèz Alès, France; [‡]Molecular Modeling Group, Swiss Institute of Bioinformatics, University of Lausanne, 1015 Lausanne, Switzerland; [§]Animalerie, Faculté de Médecine, Université de Bretagne Occidentale–Université Européenne de Bretagne, 29238 Brest, France; [¶]INSERM, U1194, Institut de Recherche en Cancérologie de Montpellier, Université de Montpellier, Institut du Cancer de Montpellier, Institut Régional du Cancer, 34298 Montpellier, France; [‖]Ludwig Center for Cancer Research, University of Lausanne, CH-1011 Lausanne, Switzerland; [#]Département d'oncologie, Université de Lausanne–Centre Hospitalier Universitaire Vaudois, CH-1011 Lausanne, Switzerland; **Centre Hospitalier Universitaire Regional, 29200 Brest, France; [††]MAT Biopharma, 91030 Evry, France; [‡‡]Immune Pharmaceuticals Inc., New York, NY 10016; [§§]Department of Biochemistry, University of Lausanne, CH-1066 Epalinges, Switzerland; and [¶¶]Biomunex Pharmaceuticals, 75006 Paris, France

[1]S.C. and J.I. contributed equally to this work.

Received for publication July 16, 2015. Accepted for publication January 28, 2016.

This work was supported by the European Commission (STREP Project BMC, Contract LSHB-CT-2005-518185), the Italian Association for Cancer Research (to J.G.), and the French National Research Agency under the program "Investissements d'avenir" Grant Agreement LabEx MAbImprove: ANR-10-LABX-5. J.G. is supported by the Italian Association for Research against Leukemia, Lymphoma, and Myeloma (Rome, Italy).

Address correspondence and reprint requests to Dr. Jean-Pierre Mach, Department of Biochemistry, University of Lausanne, Chemin des Boveresses 155, CH-1066 Epalinges, Switzerland (J.-P.M.) or Dr. Josée Golay, Centro di Terapia Cellulare "G.Lanzani,"c/o Presidio M. Rota, Via Garibaldi 11-13, 24122 Bergamo, Italy (J.G.). E-mail addresses: Jean-Pierre.Mach@unil.ch (J.-P.M.) or jgolay@asst-pg23.it (J.G.)

The online version of this article contains supplemental material.

Abbreviations used in this article: ADCC, Ab-dependent cellular cytotoxicity; BsAb, bispecific Ab; CDC, complement-dependent cytotoxicity; CFH, cysteine-free hinge; CIK, cytokine-induced killer; CLL, chronic lymphocytic leukemia; Fv, fragment variable; MM-GBSA, molecular mechanics-generalized born surface area; scFv, single-chain variable fragment; SPR, surface plasmon resonance; WT, wild-type.

www.jimmunol.org/cgi/doi/10.4049/jimmunol.1501592

More recently, several designs have in contrast aimed at producing IgG-like BsAb molecules with a functional Fc domain and greater stability. These IgG-like bispecific platforms can be either generic, applicable to any couple of Abs, or nongeneric platforms. The latter requires a two-in-one approach [i.e., selection of the binding sites that recognize two different epitopes with a high affinity (14–16)], and thus, few of these nongeneric platforms have actually been used. Among generic platforms, some approaches combine the production of recombinant Ab-derived moieties fused to specific interacting domains such as the dock-and-lock technology (17) or the Fab-arm exchange (18). Two types of IgG-like BsAbs can be distinguished, depending on whether they require dimerization of only one or two distinct H chains (19, 20). When two different H chains are used, mutation sets have to be introduced to favor the correct H chain heterodimerization (21–26). Controlling the correct pairing of the L chain with its corresponding H chain is also an important issue; this problem can be circumvented by using a common L chain (27), with the CrossMab technology (20) or using mutations at the V_H/V_L and CH/CL interfaces in Fab fragment (28).

Finally, BsAbs can have different valency. Whereas for some applications, monovalent binding to each Ag may be sufficient or advantageous (23, 27, 29), in other cases, the additional avidity or signaling potential provided by bivalent binding to both Ags is critical for the Ab biological activities (30–34).

In this paper, we describe an original generic concept allowing the generation of a new recombinant bispecific Ab format with an IgG-like structure and presenting tetrameric Ag binding sites.

Materials and Methods

Molecular modeling

We applied the Molecular Mechanics-Generalized Born Surface Area (MM-GBSA) approach (35, 36) to search for suitable mutation sites and sets of mutations that drive correct pairing of mutated H and L chains and to avoid mispairing. The crystal structure of human IgG1 anti–HIV-1 Ab B12 (Protein Data Bank code 1HZH) was used as a model. After performing the mutations with the Designer program (37), the systems were minimized using the molecular mechanics simulation package CHARMM version c31b1 (38) and the CHARMM22 force field (39). All systems (i.e., wild-type [WT], mutated matched, and mismatched pairs) were set up for Molecular Dynamics simulation with CHARMM. We also estimated the theoretical binding free energy (ΔG) using frames regularly extracted from the Molecular Dynamics simulation trajectories by applying the MM-GBSA method to identify residues making suboptimal contribution to the binding and suitable for mutations.

Cells and virus

The insect *Sf*9 cell line (ATCC catalog number CRL1711) was maintained in TC100 medium supplemented with 5% FBS (all from Life Technologies, St. Aubin, France). WT *Autographa californica* multiple nuclear polyhedrosis (*Ac*MNPV) virus clone 1.2 and recombinant baculoviruses were propagated in *Sf*9 cells.

The JOK1 5.3 cell line (JOK1 Hairy Cell Leukemia cell lines stably transduced with human CD5 cDNA) has been described previously (40). JOK1 5.3, REH acute leukemia, MOLT4, and JURKAT T cell leukemias and K562 erythroleukemia cell lines were grown in RPMI 1640 medium supplemented with 2 mM glutamine, 10% FBS (all from Euroclone, Milano, Italy) and 110 μM gentamicin (PHT Pharma, Milan, Italy). Primary chronic lymphocytic leukemia (CLL) samples were obtained after informed consent from untreated CLL patients and contained >90% CLL cells in the mononuclear fraction. The study was approved by the hospital ethical committee.

Construction of baculovirus transfer vectors

Recombinant baculoviruses expressing mutated mouse-human chimeric monospecific anti-CD5 Abs (chCD5-CR3 and chCD5-MUT4) were constructed as previously reported (41). Mutations in the CH and CL domains of H chain (pVTCg1) and L chain (pVTCK9) transfer vectors were introduced by PCR, using the primers indicated in Supplemental Table I. The cDNA encoding VH and VL domain of the anti-CD5 Ab were then inserted in these vectors giving pVTCγ1anti-CD5mutCR3 (or MUT4) and pVTCkanti-CD5mutCR3 (or MUT4).

Production of the BsAb requires the synthesis of one fused H chain and two L chains (Fig. 1). Because the duplication of sequences in baculovirus (two CH1 domains and two CL domains, both κ) generates high genome instability, two synthetic cDNA were first constructed encoding the CH1-Hinge (CH1′/Hinge 2′) and CL (CL′) domains of mAb2, but using alternative codons by hybridization of synthetic overlapping oligonucleotides (Eurogentec, Angers, France).

To generate a fused mAb1-mAb2 H chain, a linker, called A1 and encoding the amino acid sequence STPPTPSPSGG, was synthesized by hybridization of two synthetic oligonucleotides and introduced between the C terminus of mAb2 hinge (Hinge 2′) and the N terminus of mAb1 H chain. Similarly synthetic oligonucleotides were used to generate constructs encoding the fused H chain bearing two serines instead of cysteines in the hinge 2′ sequence. New transfer vector pVTchitcath was constructed to insert the cDNA encoding the fused–H chains giving pVTchitcath/anti-HLADR/A1/anti-CD5/Cγ1mutCR3 and pVTchitcath/anti-HLADR/A1/anti-CD5/Cγ1-mutMUT4 and either WT or cysteine-free hinge (CFH)2. In the same way, the L chain transfer vectors pVTPH/VLanti-CD5/CkmutCR3 and pVTPH/VLanti-CD5/CkmutMUT4 and pVTgp37/VL anti-HLADR/Ck′ were generated. All constructs were verified by sequencing.

Generation of recombinant viruses

Recombinant baculoviruses expressing WT or mutated chimeric, monospecific anti-CD5 Abs were obtained as described previously (42). For the construction of recombinant viruses expressing BsAbs, a new bacmid allowing the insertion of three genes into the viral genome was used (43), generating a triple-recombinant baculovirus coexpressing equimolar amount of the 3 chains. *Sf*9 cells were cotransfected by lipofection with transfer vectors bearing the cDNA encoding 1) the fused H chains pVTchitcath/anti-HLADR/A1/anti-CD5/Cγ1mutCR3 or MUT4 (WT or CFH), 2) the mAb2 L chain pVTgp37/VL anti-HLADR/CL′, and 3) the mAb1 L chain pVTPH/VL anti-CD5/CLmutCR3 or pVTPH/VL anti-CD5/CLmutMUT4 in the presence of purified viral DNA and DOTAP liposomal transfection reagent (Roche, Basel, Switzerland). Recombinant viruses were isolated by plaque assay, and productive clones were screened by ELISA (44). The genomic organization of recombinant viruses was controlled by Southern blotting. Sequence of integrated genes was verified after amplification by PCR and sequencing (Eurofins Genomics, Ebersberg, Germany).

Production and purification of recombinant mono- or bispecific Abs

*Sf*9 cells were seeded at a density of 6×10^5 cells/ml in 400 ml serum-free medium (SF900II; Life Technologies) in roller bottles and infected at a multiplicity of infection of 2. After 4 d incubation at 28°C, supernatant was collected, and secreted recombinant Abs were purified on protein A–Sepharose (GE HealthCare, Velizy Villacoublay, France). The concentration of purified Ab was determined using bicinchoninic acid assay, as recommended by the manufacturer (Perbio, Villebon sur Yvette/Courtaboeuf, France) using bovine IgG as a standard.

Surface plasmon resonance analysis

The surface plasmon resonance (SPR) experiments were performed on a Bia3000 apparatus according to the manufacturer's instructions (GE Healthcare). Abs were captured on anti-human Fc using Ab human Capture Kit (GE Healthcare) and different concentrations of soluble recombinant human CD5 (Life Technologies) were injected. For kinetic measurement of anti-HLA-DR Abs, use of immobilized Ag was found to be optimal. Increasing concentrations of Ab were therefore injected on biotinylated HLA-DR (TCMetrix Ltd., Epalinges, Switzerland) captured on streptavidin sensor chips. The kinetic constants were evaluated from the sensorgrams after double-blank subtraction with BioEvaluation software 3.2 (GE Healthcare) using a Langmuir 1:1 or bivalent fitting model for CD5 or HLA-DR Ag, respectively. For bispecificity analysis by sandwich-SPR assay, BsAb at 20 nM was injected on HLA-DR captured as above, followed by soluble CD5 at 120 nM. Controls included buffer instead of BsAb or CD5, to analyze BsAb dissociation with time. For bispecificity analysis by sequential-SPR assay, 100 nM CD5 was injected on BsAb captured as above, followed by 100 nM HLA-DR (or control CD5).

Binding assays

Ab binding to cells was performed by standard flow cytometry, using 1μg/ml primary Ab and a FITC-labeled anti-human Fc Ab (Sigma-Aldrich, St. Louis, MO). In some cases, inhibition experiments were performed by preincubating cells with increasing amounts of monospecific mouse anti-

CD5 and/or anti-DR Abs. Samples were analyzed in a FACSScan or FACSCantoII Instrument (BD Biosciences, San Jose, CA).

Assays for Fc-mediated immune functions

Complement-dependent cytotoxicity (CDC) was performed on JOK1 5.3 cells in the presence of 20% human serum and 10 μg/ml mono- or bispecific Ab. Cell viability was measured at 6 h with alamar blue vital dye, as described previously (45).

NK degranulation was used as a surrogate marker of ADCC (45). Briefly PBMC were plated at 1:1 ratio in presence of JOK1 5.3 cells opsonized with increasing doses of mono- or bispecific Abs. Percentage $CD107a^+/CD56^+$ cells was then measured after 4 h by flow cytometry.

For phagocytosis assays, CLL cells were stained with 0.1 μM CFSE (Molecular Probes, Thermo Scientific) and incubated with in vitro differentiated human macrophages (46), in the presence or absence of anti-CD5, bispecific, or control Abs. After 2 h incubation at 37°C, cells were harvested and stained with CD19-allophycocyanin and CD11b-PE (both BD Biosciences) and analyzed by flow cytometry (BD FACSCanto II; BD Biosciences) (47).

Redirection of T cell cytotoxicity toward a leukemia target

$CD5^+$ cytokine-induced killer (CIK) cells were generated from normal donor peripheral blood as described (48). Target cell lines were loaded with calcein-AM (Sigma-Aldrich) and incubated at a 10:1 E:T ratio, in the presence or absence of 1 μg/ml BsAb. After 4 h at 37°C, supernatant was collected, and fluorescence was measured in a fluorescence plate reader (FluoroStar Optima, BMG Labtech, Ortenberg, Germany) at 485 excitation and 520 emission. Results were measured as percentage lysis with respect to cells lysed with 1% SDS (100% lysis) after background subtraction (spontaneous calcein release).

In vivo activity

Six- to eight-week-old SCID CB-17 mice (Charles River Breeding Laboratories, Wilmington, MA), were injected i.v. with 10×10^6 JOK1 5.3 cells in PBS (10 mice per group). Mice were tail-vein injected with 0.25 mg CD5xDR-CR3 BsAb, rituximab, or irrelevant IgG1 Ab on days 3, 5, 7, and 11. Mice were monitored daily for the presence of hind-leg paralysis and in that case sacrificed. All protocols were approved by the Institutional Ethics Committee for Animal Experimentation of Brittany (authorization b-2005-SL-04) and were performed according to international regulations regarding animal experiments.

Statistical analyses

In vitro assays were analyzed using Student *t* tests, as appropriate. For in vivo data, statistical comparisons between groups were performed using factorial ANOVA. Normality and homogeneity were evaluated by Shapiro–Wilk test and the data were found to be valid.

Results

Design of BsAb

A novel chimeric tetravalent IgG_1-like BsAb is described that maintains natural Fab structures of both original mAbs as well as full human Fc. We chose, as a prototype, to direct the BsAb against human CD5 (mAb1) and human HLA-DR (mAb2) (Fig. 1). These specificities give us the opportunity to validate the BsAb activity in two different contexts, when the two Ags are carried on the same cell (i.e., JOK1 5.3 leukemia cell line or CLL cells expressing both HLA-DR and CD5) (40) or on two different cells (i.e., $HLA\text{-}DR^+$ B lymphoma cells and $CD5^+$ T-lymphocytes). The BsAb is composed of a fused H chain, carrying VH-CH1 domains of mAb1 fused in tandem with the VH-CH1-Hinge domains of mAb2 through a peptide linker. The two different mAb1 and mAb2 L chains (both κ) in contrast are free (Fig. 1).

To achieve correct pairing of the two light chains to their corresponding mAb1 and mAb2 VH-CH domains, we introduced mutations in the CH1 and CL interface of mAb1 (Fig. 1). With the help of three-dimensional structure modeling and energetic considerations, two rational modifications were proposed, the so-called charged residues and hydrophobicity-polarity-swap.

In the charged residues option, the exchange of a pair of interacting polar interface residues for a pair of neutral and salt bridge forming residues was introduced. The formation of a salt bridge can reinforce the specificity of the association, whereas an unwanted pairing should be avoided by the lack of sterical and charge complementarity between the WT and variant chains. After extensive in silico testing, the replacement of Thr^{192} by a Glu on CH1 chain and exchange of

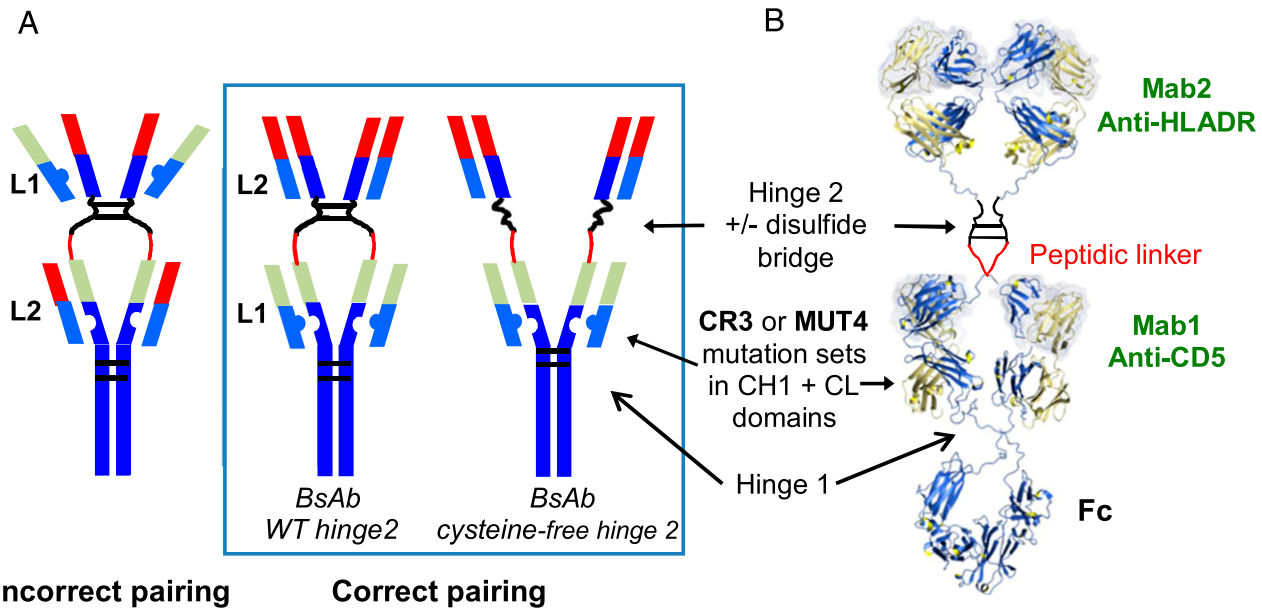

FIGURE 1. Design and three-dimensional model of the bispecific tetravalent Ab format. (A) Overall structure of the designed BsAbs bearing Fab of mAb1 and mAb2. The constant domains (CH and CL) are indicated in blue, VH/VL of mAb1 in green, and VH/VL of mAb2 in red. The hinges are in black and the peptide linker in red. *Unboxed left panel*, The risk of mispairing of the two free light chains of mAb1 and mAb2 (L1 and L2) with the fused H chain of mAb1 and 2 is shown. *Boxed panel*, The mutations introduced at the CH1/CL interface of mAb1 allow proper pairing of L1 and L2 to the fused H chain. The mutated BsAbs are presented in two formats, one with unmodified hinge 2, containing two disulfide bridges (WT hinge 2), and one with additional mutations replacing two cysteines of hinge 2 with serines, resulting in a more flexible format (cysteine-free hinge 2). (**B**) Structural modeling of the bispecific construct with WT hinge; H chain in blue and L chains in yellow.

Asn^{137} to a Lys on CL chain was chosen. These two mutated residues form a salt bridge. In addition, a substitution of Ser^{114} to Ala on CL chain was made to avoid steric clashes with a bigger lysine side chain (Fig. 2A). This mutant was named CR3 and its predicted three-dimensional structure is shown in Fig. 2B.

For the hydrophobicity-polarity-swap strategy, a double mutation was introduced on each chain: a pair of interacting apolar residues is exchanged for a pair of polar amino acids, whereas a pair of interacting polar residues is simultaneously exchanged for a pair of hydrophobic residues. After in silico testing of many potential mutations, we chose to replace the Leu^{143} of the CH1 domain by a Gln residue, whereas the facing residue of the CL chain (i.e., Val^{133}) was replaced by a Thr residue (hydrophobic to polar switch). Simultaneously, two interacting serine residues (Ser^{188} on CH1 chain and Ser^{176} on CL chain) were swapped with valine residues (polar to hydrophobic switch) (Fig. 2A). This mutant was named MUT4 and its predicted three-dimensional structure shown in Fig. 2C.

After initial testing with the Designer program (37), the binding free energies of mutated complexes, either correctly paired as well mispaired, were evaluated using the MM-GBSA method. For both CR3 and MUT4 proposed mutations, the complex between the modified CL and CH1 chains was estimated to be as stable as the WT complex, whereas significantly unfavorable interactions in the mispaired complexes were predicted. Indeed, the difference of cumulative contribution to the interaction energy of mutated residues in the properly paired and mispaired complexes was 2.0 kcal/mol in the case of hydrophobicity-polarity-swap mutant and 5.4 kcal/mol in the case of charged residues mutant.

Validation of CR3 and MUT4 mutations in mAb1

To verify the quality of the designed CR3 and MUT4 mutations (i.e., correct pairing and maintenance of Fc functionality of mutated IgG_1 H and L chains), we introduced these mutations in the anti-CD5 human-mouse chimeric mAb (chCD5, mAb1) (40), using baculovirus vectors for expression in insect cells. Glycoproteins produced in this system are functional and recombinant Abs can exhibit all effectors functions (42). Through PCR, the correct mutations were introduced into the cDNA encoding the CH1 and CL domains of anti-CD5. Recombinant baculoviruses were then generated after cotransfection of *Sf*9 cells with DNA from a defective baculovirus (BacMid) and the H and L chain transfer vectors. WT and mutant Abs were purified on protein A–Sepharose and analyzed 1) by SDS-PAGE in reducing and non-reducing conditions and 2) by size-exclusion chromatography. As shown in Fig. 3A and 3B, both mutants showed the expected migration patterns.

A

Modifications	CH1 Mab1	CL Mab1
Charged residues *CR3* mutant	Thr192Glu	Asn137Lys and Ser114Ala
Hydrophobicity-polarity swap *MUT4* mutant	Leu143Gln Ser188Val	Val133Thr Ser176Val

B

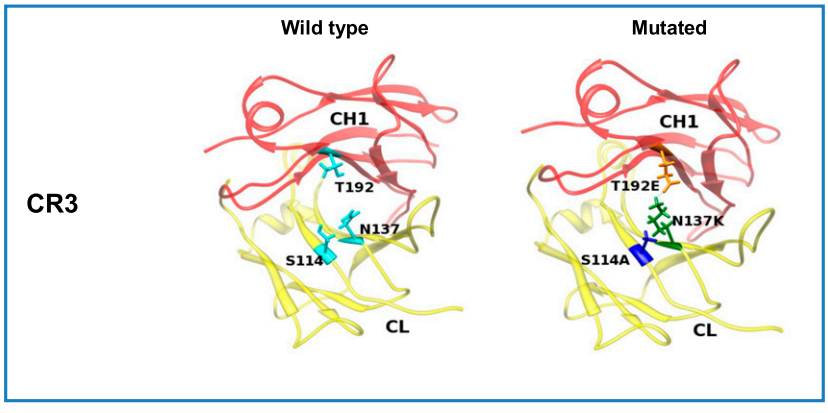

C

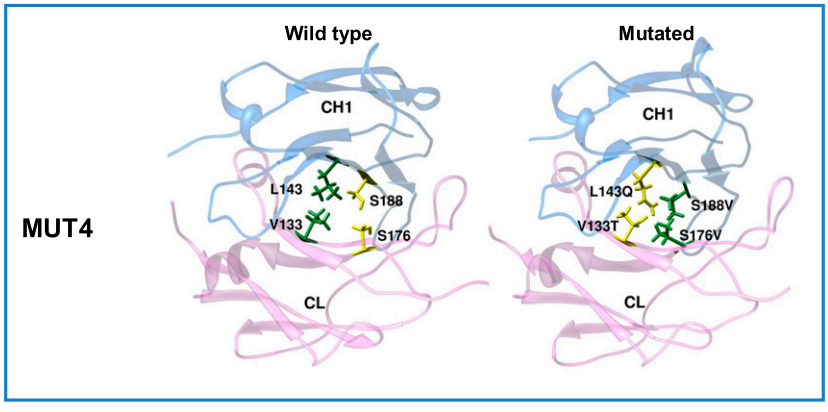

FIGURE 2. Design of specific CH and CL interface mutations. (**A**) Summary of selected mutations for each mutant. (**B**) Structural model of the CH1/CL in WT (*left*) or mutated according to the charged residues approach (CR3; *right*), showing amino acid interactions. (**C**) Structural model of the CH1/CL in WT (*left*) or mutated according to the hydrophobicity-polarity swap approach (MUT4; *right*), showing amino acid interactions.

Biacore binding assays showed that affinity of WT and mutant chCD5 for the recombinant Ag was very high in all cases (KD ranging from 3.3 to 3.7 $\times$ 10^{-12} M, very close to the apparatus limit; Table I and data not shown). Binding to natural CD5 expressed on the cell surface of the JOK1 5.3 cell line showed a similar dose response curve for WT and mutant Abs (Fig. 3C). All these data suggest correct folding of the Fab portion of anti-CD5, even in the presence of CR3 or MUT4 mutations.

We also verified whether the CR3 and MUT4 mutations affected the Fc-mediated functional activity of anti-CD5 chimeric Ab. Neither WT nor the mutant anti-CD5 Abs induced CDC in the presence of JOK1 5.3 cell line and human serum (Fig. 3D). In contrast, NK cell degranulation, as shown by induction of CD107a on $CD56^+$ cells, a surrogate marker of ADCC (Fig. 3E) (45), as well as macrophage-mediated phagocytosis of $CD5^+$ CLL target cells was induced to a similar extent by both WT or mutant anti-CD5 Abs (Fig. 3F).

Altogether, these data suggest that Fc function is unaltered by the mutations introduced in the chimeric anti-CD5 Ab CH1-CL domain. We have similarly mutated other chimeric Abs without any significant effect on Ag binding or Fc function (data not shown).

Production and characterization of CD5xDR BsAbs

The construction of the tetravalent BsAb directed against CD5 and HLA-DR (CD5xDR) was based on either the CR3 or the MUT4 format in its anti-CD5 portion (mAb1). The BsAb contained a fused H chain carrying the VH-CH1 domains from mAb1 (anti-CD5) linked in tandem to the VH-CH1-Hinge domains of mAb2 (anti–HLA-DR). For the fusion, we chose a semirigid peptide linker (A1) STPPTPSPSGG, inserted downstream from hinge sequence (Hinge 2) of mAb2 (Fig. 4A). The fused H chain was thus composed of the following domains (from N to C terminus): VH(anti–HLA-DR)-CH1(WT)-hinge2-linker(A1)-VH(anti-CD5)-CH1(either CR3 or MUT4)-hinge1-CH2-CH3. The two L chains (anti-CD5, with the appropriate CR3 or MUT4 mutations, and WT anti–HLA-DR) are expressed as separate chains (Fig. 1).

Baculoviruses expressing the recombinant CD5xDR-CR3 or -MUT4 BsAbs were generated in one step by homologous recombination after transfection of *Sf*9 cells with a defective viral DNA and the three transfer vectors bearing expression cassettes for the fused-H chain and the two L chains. The genome of the final recombinant virus is represented in Fig. 4B. Productive recombinant viruses were screened by ELISA and one clone for

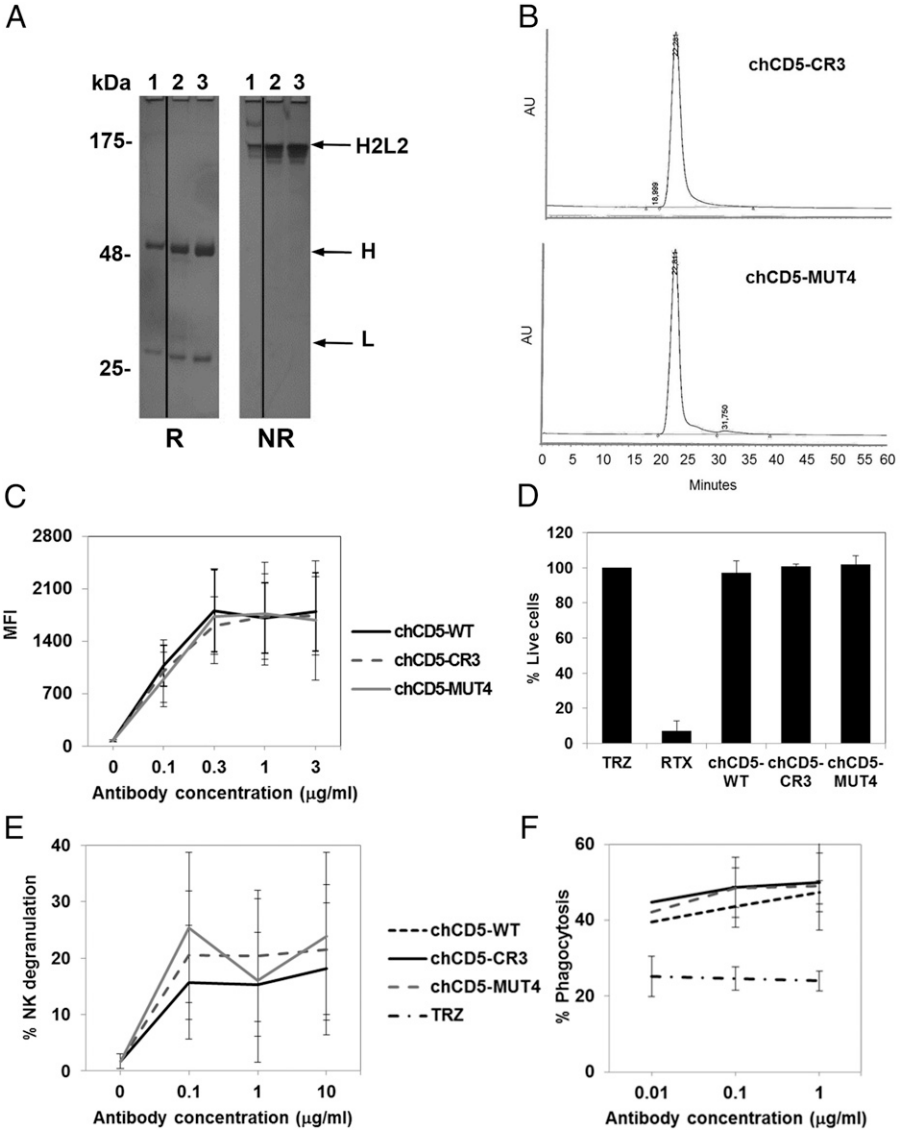

FIGURE 3. Validation of the CR3 and MUT4 mutations in the anti-CD5 monospecific chimeric Ab. (**A**) Monospecific mouse-human chimeric anti-CD5 Abs (chCD5), either WT (*lane 1*), mutated CR3 (*lane* 2), or MUT4 (*lane* 3), purified on protein A–Sepharose and analyzed by SDS-PAGE in reducing (R, *left*) and non-reducing (NR, *right*) conditions. All samples were run in parallel in a single gel, but *lane 1* (WT) was spliced and joined to *lanes 2* and *3* (mutants) during figure preparation, indicated by the black lines. (**B**) H2L2 pairing of CR3 and MUT4 chimeric anti-CD5 Abs (chCD5-CR3 and chCD5-MUT4, respectively) analyzed by size-exclusion chromatography, using 100 μg protein A–purified Abs. (**C**) Binding of increasing concentrations of chCD5-WT (black continuous lines), -CR3 (gray continuous lines), or -MUT4 (gray discontinuous line) to $CD5^+$ JOK1 5.3 cell line analyzed by flow cytometry. (**D**) Capacity of chCD5-WT, -CR3, or MUT4 at 10μg/ml to mediate CDC of JOK1 5.3 cell line measured by alamar blue assay. (**E**) Capacity of chCD5-WT, -CR3, or MUT4 at increasing concentrations to induce NK cell degranulation measured by flow cytometry. (**F**) Capacity of chCD5-WT, -CR3, -MUT4, or negative control trastuzumab (TRZ) Ab, at increasing concentrations, to mediate phagocytosis of $CD5^+$ CLL targets by macrophages, measured by flow cytometry. (C–F) The results are the means and SDs of three experiments.

Table I. Binding capacity of monospecific and bispecific Abs by surface plasmon resonance

Ab	Ag[a]	Association Rate k_a (1/Ms)	Dissociation Rate k_d (1/s)	Affinity K_D (M)
mAb				
chCD5-CR3	CD5	4.78×10^5	1.76×10^{-6}[b]	3.68×10^{-12}
chCD5-MUT4	CD5	6.08×10^5	1.99×10^{-6}[b]	3.27×10^{-12}
BsAb				
CD5xDR-CR3	CD5	2.14×10^5	1.11×10^{-4}	0.52×10^{-9}
CD5xDR-MUT4	CD5	2.72×10^5	3.21×10^{-4}	1.18×10^{-9}
CD5xDR-CR3-CFH	CD5	3.25×10^5	1.59×10^{-4}	0.49×10^{-9}
CD5xDR-MUT4-CFH	CD5	3.96×10^5	4.21×10^{-4}	1.06×10^{-9}
mAb				
chHLA-DR	HLA-DR	1.10×10^6	6.70×10^{-2}	6.10×10^{-8}
BsAb				
CD5xDR-CR3	HLA-DR	4.86×10^5	1.90×10^{-2}	3.90×10^{-8}

[a]Soluble CD5 was used with immobilized Ab. HLA-DR was immobilized on the chip.
[b]k_d values near the limit of the apparatus (5×10^{-6}/s).

each construct was used for the production-purification steps. BsAb production levels were similar to those observed during the production of monospecific Abs (10–15 mg/l at low cell density). In both cases, the size of the fused-H chain and light chains in SDS-PAGE corresponded to the calculated molecular mass: 78 and 25 kDa, respectively (Fig. 4C). Size-exclusion chromatography on Superose 6 indicated that only one molecule with the expected molecular mass (260 kDa calculated molecular mass) was produced, suggesting correct pairing with the light chains (Fig. 4D).

We next verified the binding specificity of the CD5xDR-CR3 and CD5xDR-MUT4 BsAbs on CD5 and HLA-DR–positive or –negative cell lines. As shown in Fig. 5A (*lower panels*), both BsAbs were able to specifically bind to the CD5 or HLA-DR single or double positive cell lines but not to the negative ones, demonstrating that both Ags were recognized. Furthermore we investigated whether each BsAb molecule could bind to both Ags, using a CD5/HLA-DR double-positive CLL cells and cross-blocking each Ag with mouse anti-CD5 and anti-DR. As shown in Fig. 5B (*left two panels*), a marked decrease of BsAb binding to $CD5^+DR^+$ CLL cells took place only in the presence of excess of both mouse anti-CD5 and mouse anti-DR, indicating that both these Ags are bound by the same BsAb molecules. There were no significant differences between the CR3 and MUT4 versions of BsAbs (Fig. 5B).

To investigate whether the CD5xDR BsAbs could bind to the two Ags on two different cells, we performed redirected cytotoxicity assays with cytotoxic $CD5^+$ T cells and DR^+ targets cells. As effector T cells, we used the well characterized CIK cells (48, 49). The DR^+ cell line JOK1 5.3 and the primary lymphoma cells DLBCL-PER were used as targets and the DR-negative cell line JURKAT as negative control. As shown in Fig. 5C, both CD5xDR BsAbs were able to redirect killing of CIK toward HLA-DR–positive cells. Cell killing was efficient with up to 70% cytotoxicity observed at a 10:1 E:T ratio. In contrast, BsABs did not increase significantly the background cytotoxicity directed against the HLA-DR–negative JURKAT cell line. These results demonstrate that the BsAbs can redirect $CD5^+$ CIK cells toward DR^+ targets and therefore bind the two Ags on different cells. There was no significant difference between the CR3 and MUT4 versions of CDxDR BsAbs (Fig. 5C).

In addition, we measured avidity of the CD5xDR-CR3 bispecific Ab on native Ags compared with the parent chimeric monospecific Abs. For this purpose, binding of the chimeric Abs to $CD5^+DR^+$ CLL cells was inhibited by increasing amounts of combined mouse anti-CD5 and anti-DR Abs. Fifty-percent inhibition of CD5xDR-CR3 binding (IC_{50}) was observed with ~8 nM mouse Abs, compared with an IC_{50} of 0.7 and 3 nM for chCD5 and chDR binding, respectively (Fig. 5D). This shows that the avidity of the tetravalent BsAb CD5xDR-CR3 for native Ags is higher than that of the corresponding monospecific bivalent mAbs.

Finally, we analyzed binding of the CD5xDR-CR3 BsAb on the two Ags by SPR. Binding to both recombinant CD5 and HLA-DR could be demonstrated using sequential assays as well as sandwich assay (Fig. 6). The latter further proves simultaneous binding of both Ags by the same BsAb.

Generation of cysteine-free hinge mutants and comparison of binding affinity by SPR

Because the hinge of mAb2 (called hinge 2) contains a couple of cysteines that mediate dimerization of the IgG H chains, creating a relatively rigid and closed structure of the BsAb (Fig. 1), we also constructed two additional modified CD5xDR BsAbs, in which the pair of cysteines in hinge 2 were replaced by two serines, on the same CD5xDR-CR3 or -MUT4 formats described above. These potentially more flexible BsAbs with CFHs were called CD5xDR-CR3-CFH, CD5xDR-MUT4-CFH. These new BsAb formats were produced and purified, yielding the equivalent size and purity of protein as the hinge WT versions of the Ab. Yield was ~10 mg/l at low density (data not shown).

Binding kinetics and affinities of the different BsAbs were first analyzed by SPR against soluble CD5 and compared with that of the corresponding monospecific Abs. The BsAbs showed lower affinity for CD5 compared with the monospecific Abs, mostly because of a higher dissociation rate (Table I). Comparison of the CR3 with MUT4 BsAbs showed that the kinetic constants and affinities of the two versions for CD5 were very similar, with only a slightly more favorable dissociation rate and binding affinity of CR3 compared with MUT4 BsAbs (Table I). The different hinges in the BsAbs (containing cysteines or not) did not affect binding to CD5. The affinity constants of all BsAb (KD) were quite high in all cases (10^{-9}–10^{-10}M), suggesting proper folding of these molecules (Table I).

The binding constants of the chimeric anti-DR mAb and of BsAb CD5xDR-CR3 for recombinant HLA-DR was also analyzed by SPR. The affinity of BsAb for HLA-DR was very similar to that of the parent Ab (Table I).

Comparison of biological activities of all four BsAbs constructs

We next compared the binding of all four BsAb formats to the $CD5^+DR^+$ JOK1 5.3 cell line. Dose-response curves demonstrated that CD5xDR-CR3 and CD5xDR-MUT4 have a similar binding affinity, whereas CFH versions of the same BsAbs showed slightly lower binding at all doses ($p < 0.05$ and $p < 0.01$ for CR3 and MUT4, respectively; Fig. 7A).

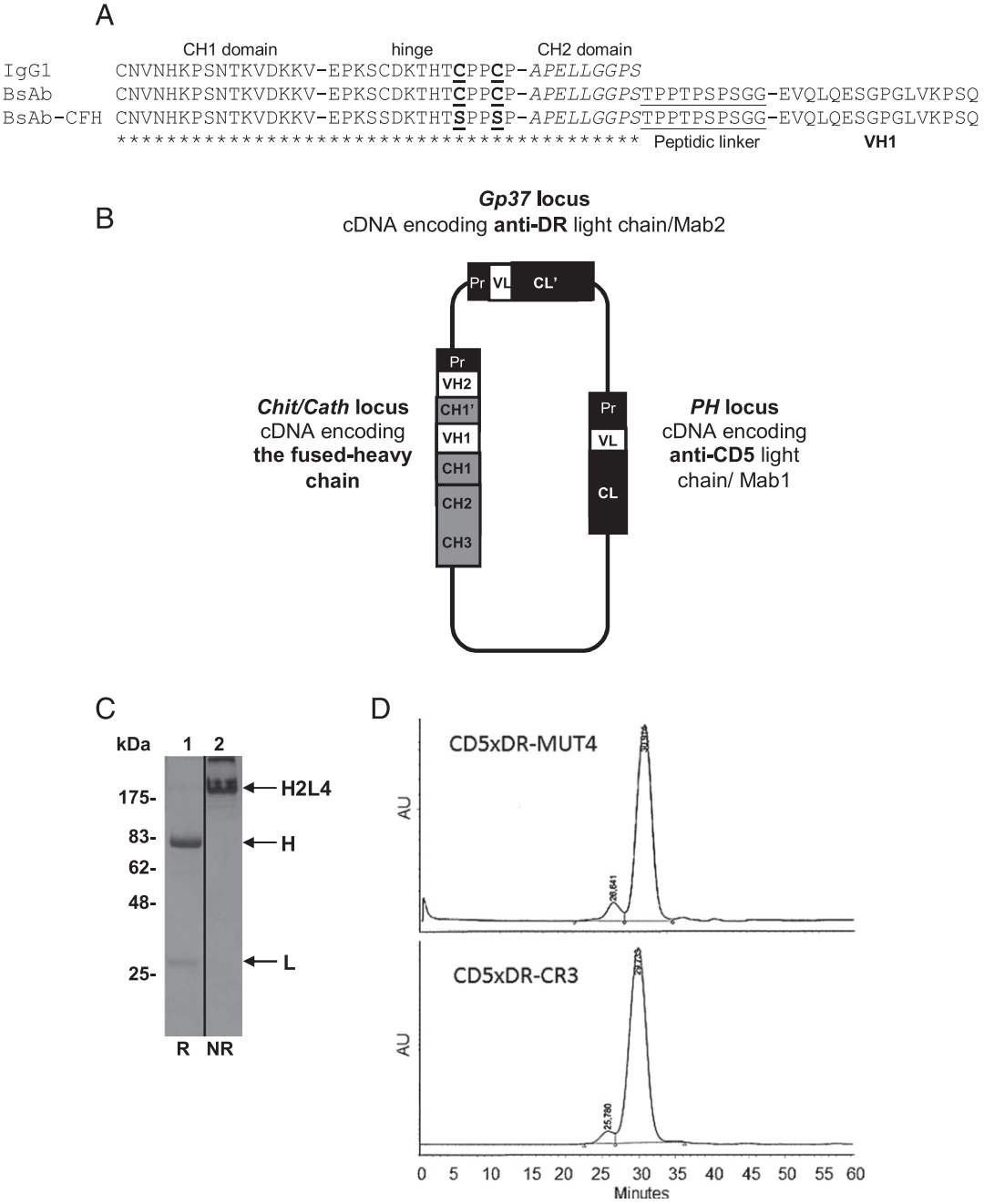

FIGURE 4. Construction of the BsAbs. (**A**) Sequences of the WT hinge of human IgG_1 H chain, aligned with that of hinge 2 and linker sequences inserted between mAb1 and mAb2 in BsAb, in the WT and CFH format. Residues engaged in disulfide bridges are underlined. (**B**) Genome organization of the recombinant virus expressing the BsAbs. CH1′, Hg2′, and CL′ represent synthetic genes for mAb2. (**C**) SDS-PAGE analysis of purified recombinant BsAb CD5xDR-MUT4. *Lane 1*, Reducing conditions (R). *Lane 2*, Nonreducing conditions (NR). The samples were run in parallel in a single gel and relevant lanes spliced and joined during figure preparation, indicated by the black lines. (**D**) Size-exclusion chromatography analysis of purified recombinant CD5xDR-MUT4 and CD5xDR-CR3 on a Superose 6 column. CH1, CH2, CH3, constant domains of human IgG_1; Hg, hinge domain of human IgG1; Pr, promoter; VH, variable domain of H chain; VL, variable domain of L chain.

We also analyzed the Fc-mediated functional activities of all four BsAb formats. All BsAbs were strong inducers of CDC, but the CFH versions were slightly less effective than the hinge 2 WT versions of BsAbs, with ~75% lysis compared with 95%, respectively (Fig. 7B). This difference was significant for both the CR3 and MUT4 formats ($p < 0.05$ and < 0.001, respectively).

All BsAbs were able to induce NK cell degranulation. We did not observe a significant difference between the different Abs (Fig. 7C). Finally, we analyzed the capacity of all four BsAb formats to mediate phagocytosis of $CD5^+DR^+$ CLL cells by macrophages. As shown in Fig. 7D, all four BsAbs mediated significant phagocytosis at 0.1–1 μg/ml BsAb.

Stability of CD5xDR-CR3 and activity in vivo

To investigate the therapeutic activity of BsAbs in vivo, we selected the CD5xDR-CR3 format, this being the most consistently active format for binding and functional effects in vitro (Fig.7, Table I). Furthermore, this format was found to be very stable in vitro even upon long-term storage. Indeed, size-exclusion chromatography analysis of a sample of CD5xDR-CR3 stored for 16 mo at 4°C in

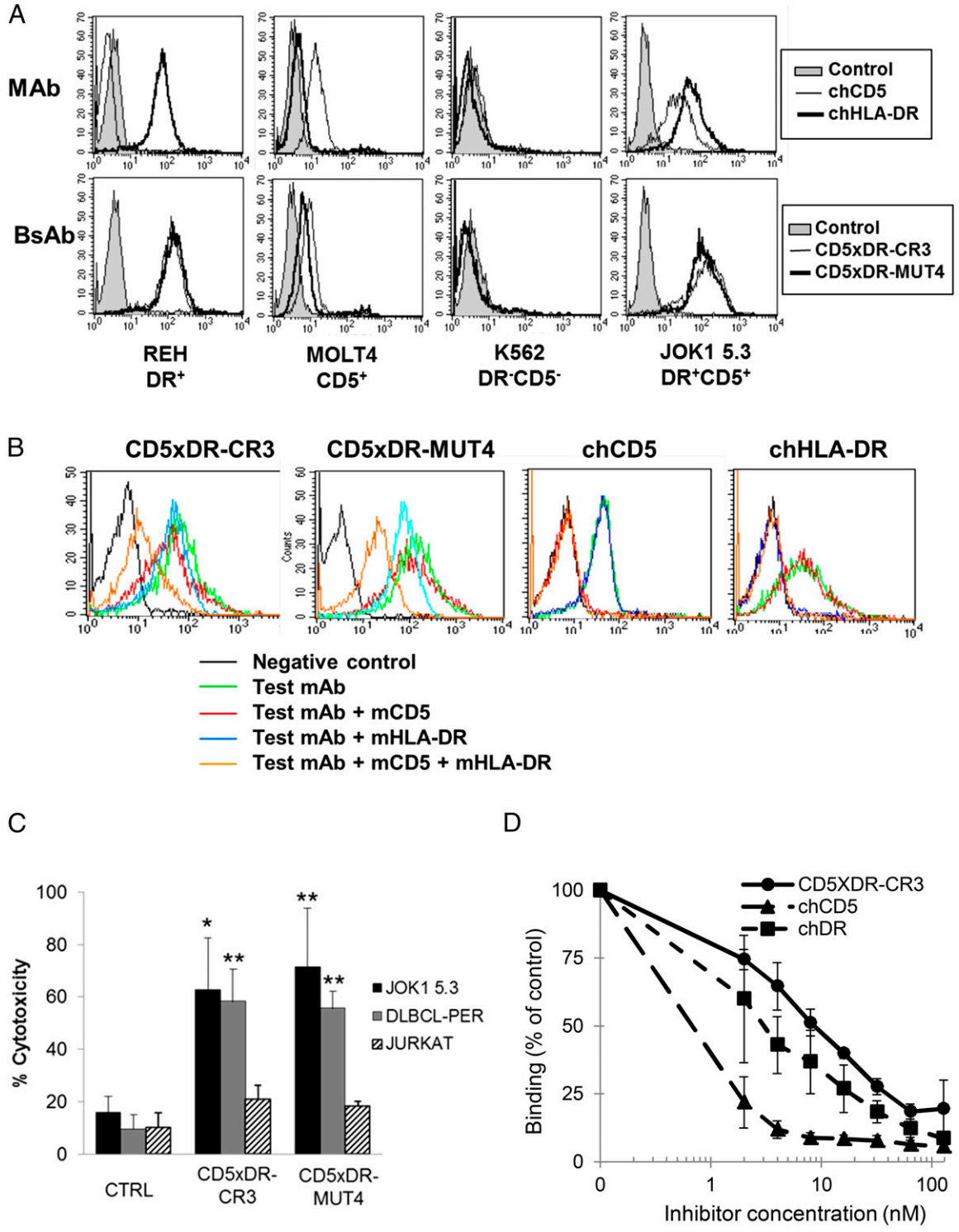

FIGURE 5. Binding of mono- or bispecific Abs to cells expressing CD5 and/or HLA-DR. (**A**) Binding of chimeric anti-CD5 and anti-HLA-DR mAbs (*upper panel*) or of BsAb CD5xDR-CR3 and CD5xDR-MUT4 (*lower panel*) to the indicated CD5 or HLA-DR–positive and –negative cell lines. (**B**) Binding inhibition experiments using $CD5^+HLA\text{-}DR^+$ CLL cells as targets and mouse anti-CD5 (mCD5) or anti-HLA-DR (mHLA-DR) mAbs at 10 μg/ml to block binding of 1 μg/ml of the indicated chimeric BsAbs or monospecific Abs. Binding was revealed with an anti–human-Fc-FITC secondary Ab. (**C**) Redirected cytotoxicity assay with $CD5^+$ CIK cells as effectors and as targets either $CD5^+DR^+$ JOK1 5.3 (black bars), $CD5^-DR^+$ DLBCL-PER cells (gray bars), or $CD5^+DR^-$ JURKAT cells (striped bars). (**D**) Binding inhibition experiments using $CD5^+HLA\text{-}DR^+$ CLL cells as targets and mouse anti-CD5 (mCD5) plus anti–HLA-DR (mHLA-DR) mAbs, at 2–128 nM each, to block binding of 4 nM tetravalent chimeric CD5xDR-CR3 BsAb, anti-CD5 (chCD5), or anti–HLA-DR (chDR), revealed with anti–human-Fc-FITC. The data show that the tetravalent BsAb has a higher avidity than the parent bivalent monospecific Abs.

20 mM Tris-HCl buffer (pH 7.4) showed that little aggregation or degradation of the protein had taken place (Fig. 8A). In confirmation of these findings, CD5xDR-CR3 was functionally fully active even after months of storage at 4˚C (JG, data not shown). We also investigated the stability of CD5xDR-CR3 in vitro when incubated at 37˚C in 100% mouse serum for 2–15 d. CD5xDR-CR3 maintained ~86, 70, and 62% binding capacity after 2, 9, and 15 d at 37˚C, respectively (Fig. 8A), indicating a good

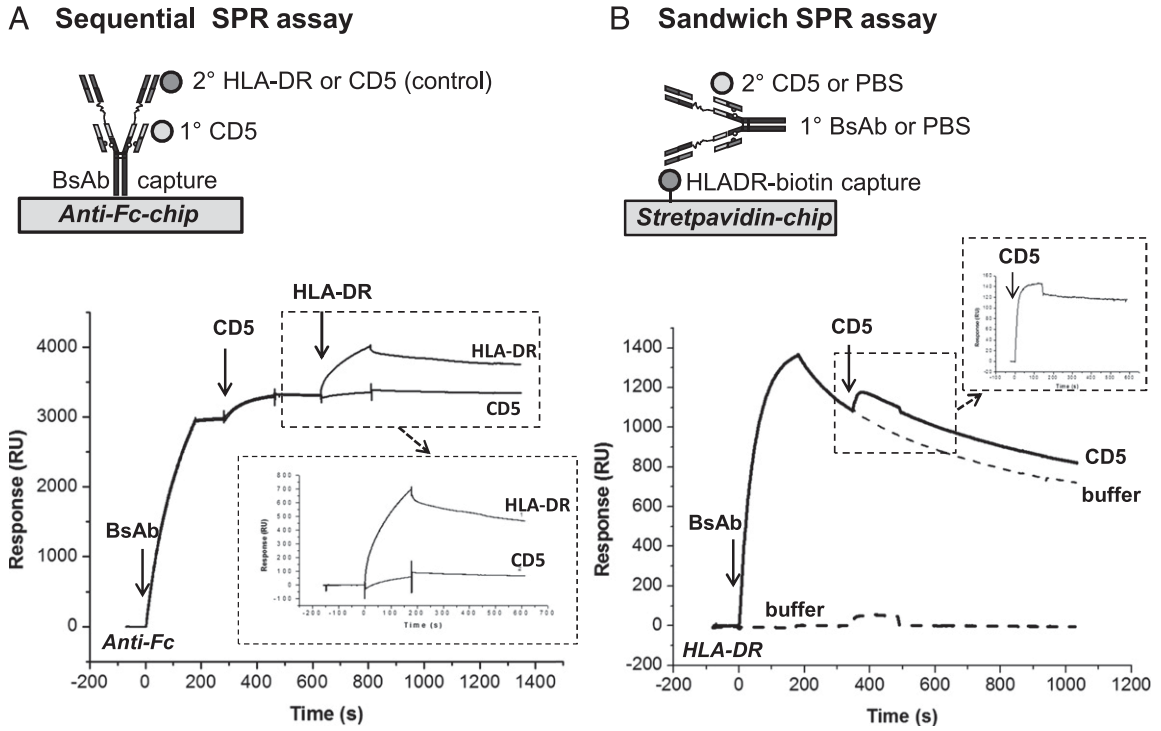

FIGURE 6. Demonstration of CD5xDR-CR3 BsAb binding to the two Ags by SPR. (**A**) Sequential SPR assay: CD5xDR-CR3 BsAb was immobilized on the chip by anti-Fc capture. CD5 protein was injected, followed by HLA-DR. The *insert* presents the enlargement of the indicated portion of the curve to better show the additional binding of HLA-DR. (**B**) Sandwich SPR assay. HLA-DR-biotin was captured on a streptavidin chip. CD5xDR-CR3 BsAb (continuous line) or buffer (dotted line) were then added, followed by CD5 (continuous line) or buffer control (dotted line). The *insert* shows the enlargement of the indicated portion of the curves, after subtraction of the buffer curve, which better illustrates the binding of CD5 to the BsAb.

stability of the molecule even in these more physiological conditions.

We finally analyzed the therapeutic activity of CD5xDR-CR3 against a $CD5^+DR^+$ leukemia target (JOK1 5.3). Tumor cells were inoculated i.v., and 0.25 mg BsAb CD5xDR-CR3 was given i.v. on days 3, 5, 7, and 11. BsAb treatment led to a 15 d delay in median survival time, compared with untreated controls (35 versus 20 d, respectively) ($p < 0.001$) (Fig. 8B). Furthermore BsAb was more effective than rituximab given at the same dose (median survival time 31 d; $p < 0.05$).

In conclusion, the generic platform described allows production of novel tetravalent BsAb format with therapeutic activity in an in vivo model of leukemia. A patent for this platform has been published (Multispecific antibodies. European patent application PCT/IB2012/053482, Publication No. WO2013005194 A2. 2013 Jan 10).

Discussion

An original platform is described that allows the synthesis of an IgG1-like bispecific tetravalent Ab molecule, carrying a complete and functional Fc. The technology consists in the introduction of paired mutations at the CH1-CL interface of a first human IgG1 Ab (mAb1), and fusing the VH-CH1 sequence of a second Ab (mAb2) at the N terminus of the H chain of the first Ab. The mAb1 CH1-CL mutations force the correct binding of the two different free light chains (CL-VL) to their respective VH-CH1 domains. Two different sets of CH1-CL interface mutations were tested in this study, called CR3 and MUT4, as well as two different hinge sequences separating the two mAbs, on a prototype CD5xDR BsAb.

The fusion of the VH-CH1 domains of mAb2 to the H chain of mAb1 is realized via a peptide linker. We have observed that the natural semiflexible A1 linker STPPTPSPSGG, placed downstream of hinge 2 sequence, conserved a full binding activity of BsAb toward soluble human CD5. Moreover, this linker is a part of the human IgA natural hinge sequence, which may also minimize the immunogenicity of the molecule.

The specific pairing between the mAb1 and mAb2 VH-CH1 domains and their corresponding L chains (CL/VL domains) was favored and stabilized by the introduction of mutations at the CH-CL interface in one of these Fab (mAb1), the other one being non-mutated (mAb2). Two mutational approaches have been chosen and designed in silico: 1) a charged residues approach (CR3 mutant) and 2) a hydrophobicity-polarity swap strategy (MUT4 mutant). Production of mutated anti-CD5 monospecific and CD5xDR bispecific Abs has demonstrated that these mutations do not affect the structure and the properties of the recombinant molecules. The two mutations did not differ significantly with each other in terms of specificity and affinity for CD5, specificity for HLA-DR or Fc functions.

In particular, binding affinity and dissociation constants to CD5 and HLA-DR were measured by SPR. Affinity of BsAbs was lower than that of monospecific anti-CD5 mAb, mostly because of higher dissociation rate. This phenomenon is probably induced by steric hindrance of mAb1 Fab, positioned internally in the bispecific molecule. Similar, albeit smaller decreases in affinity have already been reported for other BsAb formats (19, 50). Also worth noting is that the affinity for CD5 of all BsAbs tested in this study was in the 10^{-9}–10^{-10} range, which is within that observed for several other therapeutic Abs. The affinity for HLA-DR was very similar between the BsAb CR3 format compared with monospecific anti-DR Ab, suggesting correct overall folding of the molecule.

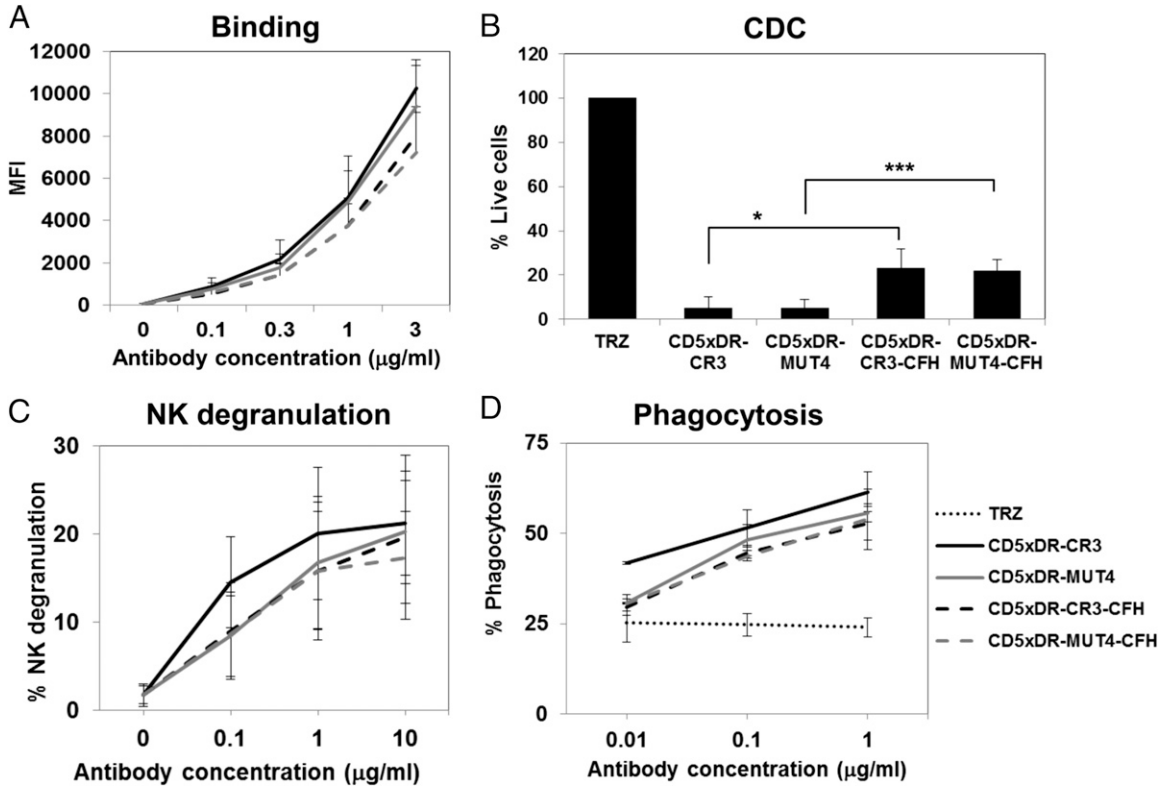

FIGURE 7. Function of the different bispecific Ab formats. Different functions of the CD5xDR-CR3 (black lines) and CD5xDR-MUT4 BsAbs (gray lines), either in the WT (continuous lines) or CFH formats (discontinuous lines) are shown. (**A**) Binding to $CD5^+DR^+$ JOK1 5.3 cell line at increasing Ab concentrations. (**B**) CDC of JOK1 5.3 with 20% human serum and 10 μg/ml indicated Abs. (**C**) Degranulation of NK cells (CD107a induction on $CD56^+$ NK cells) induced by JOK1 5.3 cells opsonized with BsAbs at increasing concentrations. (**D**) Phagocytosis by macrophages of CLL opsonized with increasing BsAb concentrations. Trastuzumab (TRZ) was also used as negative control (dotted line). The data are the means and SDs of 3 independent experiments. $*p < 0.05$, $***p < 0.001$.

Interestingly, the CD5xDR-CR3 and -MUT4 BsAbs were shown by cross-blocking experiments to bind specifically to the two different Ags expressed by the same target cell (cis binding to a $CD5^+HLA\text{-}DR^+$ CLL target). They were also shown to bind specifically to the Ags expressed by two different cells (*trans* binding to two different cellular targets), since they were able to very efficiently redirect $CD5^+$ CIK cells to kill $HLA\text{-}DR^+$ targets, with up to 70% lysis obtained at a 10:1 E:T ratio. In this context, it is worth noting that the $CD5^+$ cell line JURKAT was not killed by $CD5^+$ CIK cells in presence of BsAbs, showing that the effector has to express a different Ags (CD5) than the target (HLA-DR) for killing to occur. This is likely because of the anti-CD5 and anti-DR Fabs are placed relatively close to each other, allowing to bring the effector $CD5^+$ T cells close to the DR^+ target. Indeed, the distance between effector and target is thought to be an important parameter for redirected cell killing (51). This specificity of killing by our BsAb is an advantage, since it allows to identify different Ag pairs on effectors and targets, to redirect different killer cells to different cancer cells. Binding to the two Ags by the same CD5xDR-CR3 BsAb molecule was also demonstrated by both sequential and sandwich SPR.

The Fc portions of the different BsAbs tested in this study were fully functional in all cases and capable of mediating CDC, NK activation, as well as phagocytosis of CLL targets by macrophages. Interestingly, the CD5xDR BsAb has inherited the capacity of the monospecific recombinant anti–HLA-DR Ab to induce CDC because no CDC could be detected with the monospecific recombinant anti-CD5 Ab in the same experimental conditions. This may be due in part to higher binding of BsAb compared with anti-CD5 mAb, due to greater expression levels of HLA-DR compared with CD5.

Because the presence of disulfide bridges in the hinge 2 sequence between mAb1 and mAb2 may have imposed a relatively rigid structure, with consequent steric hindrance and reduced binding of mAb1 to CD5, we also produced two further CD5xDR BsAb molecules in which the hinge 2 cysteine residues were mutated to serine. These CFH BsAbs showed very similar properties with respect to their cysteine containing counterparts, for example equivalent binding to soluble CD5, as well as similar cell- and Fc-mediated activities (NK degranulation, phagocytosis). However CDC was reduced in the CFH formats, perhaps due to a different overall three-dimensional structure of the molecules.

Stability and aggregation are often major problems in the BsAb field because many of the molecules containing scFv or Fv domains are unstable in vitro or in vivo (i.e., proteolytic cleavage, incomplete disulfide bonds leading to partially assembled molecules) (50, 52, 53). Several strategies have been developed to stabilize these molecules, such as addition of disulfide bridges (54). Interestingly, the CD5xDR-CR3 molecule was very stable upon long-term storage in vitro at 4°C, with little formation of aggregates or degradation. It was also stable in physiological conditions, with 62% Ag binding activity maintained after 15-d incubation in mouse serum at 37°C. Finally, the in vivo experiments in mice showed that the molecule is fully functional in vivo, indicating that the molecule is stable and can activate immune-mediated mechanisms in vivo. Our platform based on natural Fab domains and WT hinges may be at the basis of the good stability, limited aggregation and in vivo functionality of the CD5xDR-CR3 format observed in this study.

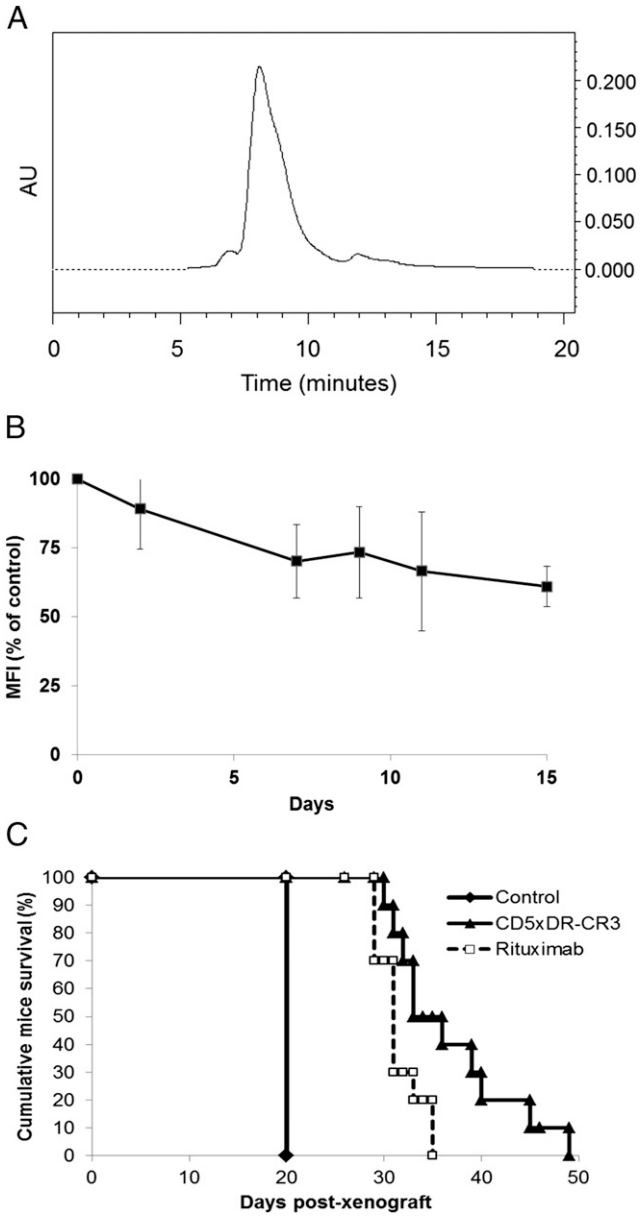

FIGURE 8. The BsAb CD5xDR-CR3 is stable in buffer or serum and active in vivo. (**A**) Size-exclusion chromatography analysis of CD5xDR-CR3 was performed, after storage of the BsAb at 1.3 mg/ml in 20 mM Tris-HCl (pH 7.4) for 16 mo at 4°C. (**B**) Stability of BsAb measured after incubation of 10 μg/ml CD5xDR-CR3 at 37°C in 100% mouse serum for up to 15 d. Functional Ab was measured at different times by binding serial dilutions of CD5xDR-CR3 to JOK1 5.3 cells and detection by indirect immunofluorescence and flow cytometry. The results are the means and SDs of three experiments at 3 μg/ml, a nonsaturating dose. (**C**) Therapeutic effect of CD5xDR-CR3 in a systemic model of $CD5^+HLA\text{-}DR^+$ leukemia (JOK1 5.3) in SCID mice. CD5xDR-CR3 (▲), rituximab (□), or negative control Ab (♦) were inoculated i.v. on days 3, 5, 7, and 11 after tumor cells and mouse survival recorded.

Few other platforms have been published that allow production of tetravalent IgG1-like molecules. Most of the other platforms make use of scFv or nanobodies linked at the N or C terminus of the L or H chains (4). scFvs often show reduced affinity/specificity compared with their parental Ab and their linking to other chains may further reduce their affinity or that of the Ab to which they are linked (32). ScFv, like nanobodies, may also show higher immunogenicity (55). Our format in contrast maintains the full structure of Fab, helping with affinity and a decrease in immunogenicity. Recently, a similar approach of modifying CH1-CL interface was taken by another group, who modified the disulphide bonds within these domains to favor correct pairing of each L chain to the proper H chain. This modification was, however, performed in the context of a bivalent, not tetravalent molecule (29).

The bispecific platform described is generic and can be applied to any Ab couple. Indeed, novel BsAbs based on this platform have already been successfully generated with specificities other than CD5 and HLA-DR (M. Duonor-Cérutti, unpublished observations). Because the platform relies on mutations introduced in the constant domains of CH1 and CL, it allows the rapid cloning of variable domains of different Abs into preformed cassettes, without the need for selection of best mutants in each case. The BsAbs produced are easily purified on protein A–Sepharose columns like standard IgGs. Furthermore, the tetravalency of the BsAbs presented in this paper may have many advantages, at least for some applications: 1) a gain of avidity/specificity, for example for target cells expressing both Ags, as shown in this paper; 2) improved apoptosis induction or growth arrest by cross-linking two different proapoptotic Ags or growth promoting molecules; and 3) the possibility to efficiently and specifically redirect immune effector cells (CIK, NK, T cells, macrophages) toward neoplastic targets. Finally, the fully functional Fc portion, in addition to greater stability, may add further immune mediated properties such as CDC, ADCC, phagocytosis, as shown in this study. Nonetheless, we have not compared our tetravalent molecules with bivalent or other tetravalent bispecific formats. So we cannot know at the present time whether this approach would be more efficient or effective than existing platforms.

The choice of the BsAb format (bi- or tetravalent, Fc bearing or not) will clearly depend on the specific application. Although Fc-mediated activities have been thought to be a disadvantage for some anticancer BsAbs because they could induce killing of effector cells, our data suggest that this is not the case for our BsAb, which does not mediate killing of $CD5^+$ effector cells. Furthermore, other BsAbs formats with highly effective Fc, like the CD3xEpCAM or CD3xCD20 TrioMabs (56, 57), have reached the clinic and appear to have very interesting clinical activities in vivo. Further work will be required in vitro and in vivo, to investigate the advantage of maintaining a fully functional Fc in our BsAb format, according to the specific targets chosen. If necessary, an Fc unable to bind to FcγRs, or on the contrary, an Ab more active in binding specific FcγRs could also be designed on our platform through point mutations or glycoengineering (58). Finally, the technology presented in this study is also applicable to the production of tetravalent monospecific Abs, which could be highly efficient in the clustering of membrane receptors thus enhancing the Ab efficiency, as demonstrated with multivalent anti-CD20 (31, 59, 60).

Acknowledgments

We thank Olga Pedrini, Emanuela Benzoni, Luca Bologna, Elisa Gotti and Michela Bonzi for performing in vitro experiments. We also thank the Vital-IT (http://www.vital-it.ch) Center for high-performance computing of the SIB Swiss Institute of Bioinformatics. We thank Dr. A. Bastone (Mario Negri Institute of Pharmacological Research, Milan, Italy) for performing size exclusion chromatography experiments with BsAbs.

Disclosures

J.K., J.-P.M., O.M., V.Z., J.I., M.D.-C., S.C., and J.G. are coinventors of the patent (Multispecific antibodies) relating to the molecule presented. J.K. is scientific adviser and cofounder of Immune Pharmaceuticals, Inc. and J.-P.M. is scientific adviser and cofounder of Biomunex Pharmaceuticals. The other authors have no financial conflicts of interest.

References

1. Sliwkowski, M. X., and I. Mellman. 2013. Antibody therapeutics in cancer. *Science* 341: 1192–1198.
2. Mullard, A. 2013. Maturing antibody-drug conjugate pipeline hits 30. *Nat. Rev. Drug Discov.* 12: 329–332.
3. Weidle, U. H., R. E. Kontermann, and U. Brinkmann. 2014. Tumor-antigen-binding bispecific antibodies for cancer treatment. *Semin. Oncol.* 41: 653–660.
4. Spiess, C., Q. Zhai, and P. J. Carter. 2015. Alternative molecular formats and therapeutic applications for bispecific antibodies. *Mol. Immunol.* 67(2 Pt A): 95–106.
5. Graziano, R. F., and P. Guptill. 2004. Chemical production of bispecific antibodies. *Methods Mol. Biol.* 283: 71–85.
6. Doppalapudi, V. R., J. Huang, D. Liu, P. Jin, B. Liu, L. Li, J. Desharnais, C. Hagen, N. J. Levin, M. J. Shields, et al. 2010. Chemical generation of bispecific antibodies. *Proc. Natl. Acad. Sci. USA* 107: 22611–22616.
7. Kontsekova, E., A. Kolcunova, and P. Kontsek. 1992. Quadroma-secreted bi (interferon alpha 2–peroxidase) specific antibody suitable for one-step immunoassay. *Hybridoma* 11: 461–468.
8. Kontermann, R. E. 2012. Dual targeting strategies with bispecific antibodies. *MAbs* 4: 182–197.
9. Dreier, T., G. Lorenczewski, C. Brandl, P. Hoffmann, U. Syring, F. Hanakam, P. Kufer, G. Riethmuller, R. Bargou, and P. A. Baeuerle. 2002. Extremely potent, rapid and costimulation-independent cytotoxic T-cell response against lymphoma cells catalyzed by a single-chain bispecific antibody. *Int. J. Cancer* 100: 690–697.
10. Topp, M. S., P. Kufer, N. Gökbuget, M. Goebeler, M. Klinger, S. Neumann, H. A. Horst, T. Raff, A. Viardot, M. Schmid, et al. 2011. Targeted therapy with the T-cell-engaging antibody blinatumomab of chemotherapy-refractory minimal residual disease in B-lineage acute lymphoblastic leukemia patients results in high response rate and prolonged leukemia-free survival. *J. Clin. Oncol.* 29: 2493–2498.
11. Kipriyanov, S. M., G. Moldenhauer, J. Schuhmacher, B. Cochlovius, C. W. Von der Lieth, E. R. Matys, and M. Little. 1999. Bispecific tandem diabody for tumor therapy with improved antigen binding and pharmacokinetics. *J. Mol. Biol.* 293: 41–56.
12. Johnson, S., S. Burke, L. Huang, S. Gorlatov, H. Li, W. Wang, W. Zhang, N. Tuaillon, J. Rainey, B. Barat, et al. 2010. Effector cell recruitment with novel Fv-based dual-affinity re-targeting protein leads to potent tumor cytolysis and in vivo B-cell depletion. *J. Mol. Biol.* 399: 436–449.
13. Els Conrath, K., M. Lauwereys, L. Wyns, and S. Muyldermans. 2001. Camel single-domain antibodies as modular building units in bispecific and bivalent antibody constructs. *J. Biol. Chem.* 276: 7346–7350.
14. Bostrom, J., S. F. Yu, D. Kan, B. A. Appleton, C. V. Lee, K. Billeci, W. Man, F. Peale, S. Ross, C. Wiesmann, and G. Fuh. 2009. Variants of the antibody herceptin that interact with HER2 and VEGF at the antigen binding site. *Science* 323: 1610–1614.
15. Hu, S., W. Fu, W. Xu, Y. Yang, M. Cruz, S. D. Berezov, D. Jorissen, H. Takeda, and W. Zhu. 2015. Four-in-one antibodies have superior cancer inhibitory activity against EGFR, HER2, HER3, and VEGF through disruption of HER/MET crosstalk. *Cancer Res.* 75: 159–170.
16. Wozniak-Knopp, G., S. Bartl, A. Bauer, M. Mostageer, M. Woisetschläger, B. Antes, K. Ettl, M. Kainer, G. Weberhofer, S. Wiederkum, et al. 2010. Introducing antigen-binding sites in structural loops of immunoglobulin constant domains: Fc fragments with engineered HER2/neu-binding sites and antibody properties. *Protein Eng. Des. Sel.* 23: 289–297.
17. Rossi, E. A., D. M. Goldenberg, and C. H. Chang. 2012. The dock-and-lock method combines recombinant engineering with site-specific covalent conjugation to generate multifunctional structures. *Bioconjug. Chem.* 23: 309–323.
18. Labrijn, A. F., J. I. Meesters, B. E. de Goeij, E. T. van den Bremer, J. Neijssen, M. D. van Kampen, K. Strumane, S. Verploegen, A. Kundu, M. J. Gramer, et al. 2013. Efficient generation of stable bispecific IgG1 by controlled Fab-arm exchange. *Proc. Natl. Acad. Sci. USA* 110: 5145–5150.
19. Wu, C., H. Ying, C. Grinnell, S. Bryant, R. Miller, A. Clabbers, S. Bose, D. McCarthy, R. R. Zhu, L. Santora, et al. 2007. Simultaneous targeting of multiple disease mediators by a dual-variable-domain immunoglobulin. *Nat. Biotechnol.* 25: 1290–1297.
20. Schaefer, W., J. T. Regula, M. Bähner, J. Schanzer, R. Croasdale, H. Dürr, C. Gassner, G. Georges, H. Kettenberger, S. Imhof-Jung, et al. 2011. Immunoglobulin domain crossover as a generic approach for the production of bispecific IgG antibodies. *Proc. Natl. Acad. Sci. USA* 108: 11187–11192.
21. Ridgway, J. B., L. G. Presta, and P. Carter. 1996. 'Knobs-into-holes' engineering of antibody CH3 domains for heavy chain heterodimerization. *Protein Eng.* 9: 617–621.
22. Atwell, S., J. B. Ridgway, J. A. Wells, and P. Carter. 1997. Stable heterodimers from remodeling the domain interface of a homodimer using a phage display library. *J. Mol. Biol.* 270: 26–35.
23. Moore, G. L., C. Bautista, E. Pong, D. H. Nguyen, J. Jacinto, A. Eivazi, U. S. Muchhal, S. Karki, S. Y. Chu, and G. A. Lazar. 2011. A novel bispecific antibody format enables simultaneous bivalent and monovalent co-engagement of distinct target antigens. *MAbs* 3: 546–557.
24. Gunasekaran, K., M. Pentony, M. Shen, L. Garrett, C. Forte, A. Woodward, S. B. Ng, T. Born, M. Retter, K. Manchulenko, et al. 2010. Enhancing antibody Fc heterodimer formation through electrostatic steering effects: applications to bispecific molecules and monovalent IgG. *J. Biol. Chem.* 285: 19637–19646.
25. Strop, P., W. H. Ho, L. M. Boustany, Y. N. Abdiche, K. C. Lindquist, S. E. Farias, M. Rickert, C. T. Appah, E. Pascua, T. Radcliffe, et al. 2012. Generating bispecific human IgG1 and IgG2 antibodies from any antibody pair. *J. Mol. Biol.* 420: 204–219.
26. Davis, J. H., C. Aperlo, Y. Li, E. Kurosawa, Y. Lan, K. M. Lo, and J. S. Huston. 2010. SEEDbodies: fusion proteins based on strand-exchange engineered domain (SEED) CH3 heterodimers in an Fc analogue platform for asymmetric binders or immunofusions and bispecific antibodies. *Protein Eng. Des. Sel.* 23: 195–202.
27. Merchant, A. M., Z. Zhu, J. Q. Yuan, A. Goddard, C. W. Adams, L. G. Presta, and P. Carter. 1998. An efficient route to human bispecific IgG. *Nat. Biotechnol.* 16: 677–681.
28. Das, R., and D. Baker. 2008. Macromolecular modeling with rosetta. *Annu. Rev. Biochem.* 77: 363–382.
29. Mazor, Y., V. Oganesyan, C. Yang, A. Hansen, J. Wang, H. Liu, K. Sachsenmeier, M. Carlson, D. V. Gadre, M. J. Borrok, et al. 2015. Improving target cell specificity using a novel monovalent bispecific IgG design. *MAbs* 7: 377–389.
30. Rudnick, S. I., and G. P. Adams. 2009. Affinity and avidity in antibody-based tumor targeting. *Cancer Biother. Radiopharm.* 24: 155–161.
31. Rossi, E. A., D. M. Goldenberg, T. M. Cardillo, R. Stein, Y. Wang, and C. H. Chang. 2008. Novel designs of multivalent anti-CD20 humanized antibodies as improved lymphoma therapeutics. *Cancer Res.* 68: 8384–8392.
32. Shahied, L. S., Y. Tang, R. K. Alpaugh, R. Somer, D. Greenspon, and L. M. Weiner. 2004. Bispecific minibodies targeting HER2/neu and CD16 exhibit improved tumor lysis when placed in a divalent tumor antigen binding format. *J. Biol. Chem.* 279: 53907–53914.
33. Ghetie, M.-A., H. Bright, and E. S. Vitetta. 2001. Homodimers but not monomers of Rituxan (chimeric anti-CD20) induce apoptosis in human B-lymphoma cells and synergize with a chemotherapeutic agent and an immunotoxin. *Blood* 97: 1392–1398.
34. Li, B., S. Shi, W. Qian, L. Zhao, D. Zhang, S. Hou, L. Zheng, J. Dai, J. Zhao, H. Wang, and Y. Guo. 2008. Development of novel tetravalent anti-CD20 antibodies with potent antitumor activity. *Cancer Res.* 68: 2400–2408.
35. Gohlke, H., and D. A. Case. 2004. Converging free energy estimates: MM-PB (GB)SA studies on the protein-protein complex Ras-Raf. *J. Comput. Chem.* 25: 238–250.
36. Zoete, V., and O. Michielin. 2007. Comparison between computational alanine scanning and per-residue binding free energy decomposition for protein-protein association using MM-GBSA: application to the TCR-p-MHC complex. *Proteins* 67: 1026–1047.
37. Wernisch, L., S. Hery, and S. J. Wodak. 2000. Automatic protein design with all atom force-fields by exact and heuristic optimization. *J. Mol. Biol.* 301: 713–736.
38. Brooks, B. R., C. L. Brooks, III, A. D. Mackerell, Jr., L. Nilsson, R. J. Petrella, B. Roux, Y. Won, G. Archontis, C. Bartels, S. Boresch, et al. 2009. CHARMM: the biomolecular simulation program. *J. Comput. Chem.* 30: 1545–1614.
39. MacKerell, A. D., D. Bashford, M. Bellott, R. L. Dunbrack, J. D. Evanseck, M. J. Field, S. Fischer, J. Gao, H. Guo, S. Ha, et al. 1998. All-atom empirical potential for molecular modeling and dynamics studies of proteins. *J. Phys. Chem. B* 102: 3586–3616.
40. Loisel, S., P. A. André, J. Golay, F. Buchegger, J. Kadouche, M. Cérutti, L. Bologna, M. Kosinski, D. Viertl, A. B. Delaloye, et al. 2011. Antitumour effects of single or combined monoclonal antibodies directed against membrane antigens expressed by human B cells leukaemia. *Mol. Cancer* 10: 42.
41. Poul, M. A., M. Cerutti, H. Chaabihi, M. Ticchioni, F. X. Deramoudt, A. Bernard, G. Devauchelle, M. Kaczorek, and M. P. Lefranc. 1995. Cassette baculovirus vectors for the production of chimeric, humanized, or human antibodies in insect cells. *Eur. J. Immunol.* 25: 2005–2009.
42. Cérutti, M., and J. Golay. 2012. Lepidopteran cells, an alternative for the production of recombinant antibodies? *MAbs* 4: 294–309.
43. Juliant, S., M. Lévêque, P. Cérutti, A. Ozil, S. Choblet, M. L. Violet, M. C. Slomianny, A. Harduin-Lepers, and M. Cérutti. 2013. Engineering the baculovirus genome to produce galactosylated antibodies in lepidopteran cells. *Methods Mol. Biol.* 988: 59–77.
44. Bès, C., L. Briant-Longuet, M. Cerutti, F. Heitz, S. Troadec, M. Pugnière, F. Roquet, F. Molina, F. Casset, D. Bresson, et al. 2003. Mapping the paratope of anti-CD4 recombinant Fab 13B8.2 by combining parallel peptide synthesis and site-directed mutagenesis. *J. Biol. Chem.* 278: 14265–14273.
45. Bologna, L., E. Gotti, M. Manganini, A. Rambaldi, T. Intermesoli, M. Introna, and J. Golay. 2011. Mechanism of action of type II, glycoengineered, anti-CD20 monoclonal antibody GA101 in B-chronic lymphocytic leukemia whole blood assays in comparison with rituximab and alemtuzumab. *J. Immunol.* 186: 3762–3769.
46. Leidi, M., E. Gotti, L. Bologna, E. Miranda, M. Rimoldi, A. Sica, M. Roncalli, G. A. Palumbo, M. Introna, and J. Golay. 2009. M2 macrophages phagocytose rituximab-opsonized leukemic targets more efficiently than m1 cells in vitro. *J. Immunol.* 182: 4415–4422.
47. Da Roit, F., P. J. Engelberts, R. P. Taylor, E. C. Breij, G. Gritti, A. Rambaldi, M. Introna, P. W. Parren, F. J. Beurskens, and J. Golay. 2015. Ibrutinib interferes with the cell-mediated anti-tumor activities of therapeutic CD20 antibodies: implications for combination therapy. *Haematologica* 100: 77–86.
48. Pievani, A., G. Borleri, D. Pende, L. Moretta, A. Rambaldi, J. Golay, and M. Introna. 2011. Dual-functional capability of $CD3^+CD56^+$ CIK cells, a T-cell subset that acquires NK function and retains TCR-mediated specific cytotoxicity. *Blood* 118: 3301–3310.
49. Introna, M., A. Algarotti, C. Micò, A. Grassi, A. Pievani, G. Borleri, J. Golay, I. Cavattoni, S. Cortelazzo, and A. Rambaldi 2011. A phase II study of sequential administration of DLI and cytokine induced killer (CIK) cells in patients with

hematologic malignancies relapsing after allogeneic hematopoietic stem cell transplantation: preliminary results. *Blood* 118: 657.
50. Shen, J., M. D. Vil, X. Jimenez, M. Iacolina, H. Zhang, and Z. Zhu. 2006. Single variable domain-IgG fusion. A novel recombinant approach to Fc domain-containing bispecific antibodies. *J. Biol. Chem.* 281: 10706–10714.
51. Bluemel, C., S. Hausmann, P. Fluhr, M. Sriskandarajah, W. B. Stallcup, P. A. Baeuerle, and P. Kufer. 2010. Epitope distance to the target cell membrane and antigen size determine the potency of T cell-mediated lysis by BiTE antibodies specific for a large melanoma surface antigen. *Cancer Immunol. Immunother.* 59: 1197–1209.
52. Orcutt, K. D., M. E. Ackerman, M. Cieslewicz, E. Quiroz, A. L. Slusarczyk, J. V. Frangioni, and K. D. Wittrup. 2010. A modular IgG-scFv bispecific antibody topology. *Protein Eng. Des. Sel.* 23: 221–228.
53. Shen, J., M. D. Vil, X. Jimenez, H. Zhang, M. Iacolina, V. Mangalampalli, P. Balderes, D. L. Ludwig, and Z. Zhu. 2007. Single variable domain antibody as a versatile building block for the construction of IgG-like bispecific antibodies. *J. Immunol. Methods* 318: 65–74.
54. Reiter, Y., U. Brinkmann, B. Lee, and I. Pastan. 1996. Engineering antibody Fv fragments for cancer detection and therapy: disulfide-stabilized Fv fragments. *Nat. Biotechnol.* 14: 1239–1245.
55. Vaneycken, I., J. Govaert, C. Vincke, V. Caveliers, T. Lahoutte, P. De Baetselier, G. Raes, A. Bossuyt, S. Muyldermans, and N. Devoogdt. 2010. In vitro analysis and in vivo tumor targeting of a humanized, grafted nanobody in mice using pinhole SPECT/micro-CT. *J. Nucl. Med.* 51: 1099–1106.
56. Ott, M. G., F. Marmé, G. Moldenhauer, H. Lindhofer, M. Hennig, R. Spannagl, M. M. Essing, R. Linke, and D. Seimetz. 2012. Humoral response to catumaxomab correlates with clinical outcome: results of the pivotal phase II/III study in patients with malignant ascites. *Int. J. Cancer* 130: 2195–2203.
57. Buhmann, R., S. Michael, H. Juergen, L. Horst, C. Peschel, and H. J. Kolb. 2013. Immunotherapy with FBTA05 (Bi20), a trifunctional bispecific anti-CD3 x anti-CD20 antibody and donor lymphocyte infusion (DLI) in relapsed or refractory B-cell lymphoma after allogeneic stem cell transplantation: study protocol of an investigator-driven, open-label, non-randomized, uncontrolled, dose-escalating Phase I/II-trial. *J. Transl. Med.* 11: 160.
58. Schanzer, J. M., K. Wartha, R. Croasdale, S. Moser, K. P. Künkele, C. Ries, W. Scheuer, H. Duerr, S. Pompiati, J. Pollman, et al. 2014. A novel glycoengineered bispecific antibody format for targeted inhibition of epidermal growth factor receptor (EGFR) and insulin-like growth factor receptor type I (IGF-1R) demonstrating unique molecular properties. *J. Biol. Chem.* 289: 18693–18706.
59. Rossi, E. A., D. M. Goldenberg, T. M. Cardillo, R. Stein, and C. H. Chang. 2009. Hexavalent bispecific antibodies represent a new class of anticancer therapeutics: 1. Properties of anti-CD20/CD22 antibodies in lymphoma. *Blood* 113: 6161–6171.
60. Gupta, P., D. M. Goldenberg, E. A. Rossi, and C. H. Chang. 2010. Multiple signaling pathways induced by hexavalent, monospecific, anti-CD20 and hexavalent, bispecific, anti-CD20/CD22 humanized antibodies correlate with enhanced toxicity to B-cell lymphomas and leukemias. *Blood* 116: 3258–3267.